

A. Equations, parameters and compartments

PBPK model equations

The following equations describe the transport of labelled (indexed with *) and unlabelled peptide via blood flow, extravasation, binding, internalization, degradation and release, excretion and radioactive decay. For therapy the peptide was intravenously injected as a 20 min infusion. The PET tracer was injected as a bolus. The variables are defined in Table A.1.

Bound and internalized peptide:

Parotid, submandibular and lacrimal glands, tumour, kidneys, liver, spleen, GI and prostate:

Constraint for total PSMA receptors $R_{0,i}$ (saturable binding)

$$R_{0,i} = R_i + RP_i + RP_i^* \quad (1)$$

Internalized peptide

$$\begin{aligned} \frac{d}{dt} P_{\text{intern},i} &= \lambda_{\text{int},i} \cdot RP_i - \lambda_{\text{release},i} \cdot P_{\text{intern},i} + \lambda_{\text{phy}} \cdot P_{\text{intern},i}^* \\ \frac{d}{dt} P_{\text{intern},i}^* &= \lambda_{\text{int},i} \cdot RP_i^* - \lambda_{\text{release},i} \cdot P_{\text{intern},i}^* - \lambda_{\text{phy}} \cdot P_{\text{intern},i}^* \end{aligned} \quad (2)$$

Bound peptide on cell surface

$$\begin{aligned} \frac{d}{dt} RP_i &= k_{\text{on}} \cdot P_{i,\text{int}} \cdot \frac{R_i}{V_{i,\text{int}}} - (k_{\text{off}} + \lambda_{\text{int},i}) \cdot RP_i + \lambda_{\text{phy}} \cdot RP_i^* \\ \frac{d}{dt} RP_i^* &= k_{\text{on}} \cdot P_{i,\text{int}}^* \cdot \frac{R_i}{V_{i,\text{int}}} - (k_{\text{off}} + \lambda_{\text{int},i}) \cdot RP_i^* - \lambda_{\text{phy}} \cdot RP_i^* \end{aligned} \quad (3)$$

Free peptide, vascular:

Transcapillary extravasation is described by the permeability surface product (PS_i) and the vascular ($V_{i,v}$) and interstitial volumes ($V_{i,int}$) of the pertaining tissue. Convection from the vascular to the interstitial space is neglected as the used peptide represents a rather small molecule (I).

All tissues except kidneys and lungs

$$\begin{aligned}\frac{d}{dt} P_{i,v} &= PS_i \left(\frac{P_{i,int}}{V_{i,int}} - \frac{P_{i,v}}{V_{i,v}} \right) + F_i \left(\frac{P_{ART}}{V_{ART}} - \frac{P_{i,v}}{V_{i,v}} \right) + \lambda_{phy} \cdot P_{i,v} \\ \frac{d}{dt} P_{i,v}^* &= PS_i \left(\frac{P_{i,int}^*}{V_{i,int}} - \frac{P_{i,v}^*}{V_{i,v}} \right) + F_i \left(\frac{P_{ART}^*}{V_{ART}} - \frac{P_{i,v}^*}{V_{i,v}} \right) - \lambda_{phy} \cdot P_{i,v}^*\end{aligned}\tag{4}$$

For brain $PS = 0$

Lungs

$$\begin{aligned}\frac{d}{dt} P_{LU,v} &= PS_{LU} \left(\frac{P_{LU,int}}{V_{LU,int}} - \frac{P_{LU,v}}{V_{LU,v}} \right) + F \left(\frac{P_{VEN}}{V_{VEN}} - \frac{P_{LU,v}}{V_{LU,v}} \right) + \lambda_{phy} \cdot P_{LU,v} \\ \frac{d}{dt} P_{LU,v}^* &= PS_{LU} \left(\frac{P_{LU,int}^*}{V_{LU,int}} - \frac{P_{LU,v}^*}{V_{LU,v}} \right) + F \left(\frac{P_{VEN}}{V_{VEN}} - \frac{P_{LU,v}^*}{V_{LU,v}} \right) - \lambda_{phy} \cdot P_{LU,v}^*\end{aligned}\tag{5}$$

Kidneys

$$\begin{aligned}\frac{d}{dt} P_{K,v} &= -\frac{P_{K,v}}{V_{K,v}} \cdot (F_{fil} + F_K) + \frac{F_K}{V_{ART}} \cdot P_{ART} + \frac{P_{intra,K}}{V_{intra,K}} \cdot (F_{fil} - F_{ex}) + \lambda_{phy} \cdot P_{K,v}^* \\ \frac{d}{dt} P_{K,v}^* &= -\frac{P_{K,v}^*}{V_{K,v}} \cdot (F_{fil} + F_K) + \frac{F_K}{V_{ART}} \cdot P_{ART}^* + \frac{P_{intra,K}^*}{V_{intra,K}} \cdot (F_{fil} - F_{ex}) - \lambda_{phy} \cdot P_{K,v}^*\end{aligned}\quad (6)$$

Veins

$$\begin{aligned}\frac{d}{dt} P_{VEN} &= -k_{Pr} \cdot P_{VEN} + \sum \frac{F_i}{V_i} P_{i,v} - \frac{F_M}{V_M} P_{M,v} - \frac{F_{GL}}{V_{GL}} P_{GL,v} + \frac{F_M + F_{GL}}{V_L} P_{L,v} + \lambda_{phy} \cdot P_{VEN}^* \\ \frac{d}{dt} P_{VEN}^* &= -k_{Pr} \cdot P_{VEN}^* + \sum \frac{F_i}{V_i} P_{i,v}^* - \frac{F_M}{V_M} P_{M,v}^* - \frac{F_{GL}}{V_{GL}} P_{GL,v}^* + \frac{F_M + F_{GL}}{V_L} P_{L,v}^* - \lambda_{phy} \cdot P_{VEN}^*\end{aligned}\quad (7)$$

Arteries

$$\begin{aligned}\frac{d}{dt} P_{ART} &= -\sum \frac{F_i}{V_{ART}} \cdot P_{i,v} + \frac{F}{V_{LU,v}} \cdot P_{LU,v} + \lambda_{phy} \cdot P_{ART}^* \\ \frac{d}{dt} P_{ART}^* &= -\sum \frac{F_i}{V_{ART}} \cdot P_{i,v}^* + \frac{F}{V_{LU,v}} \cdot P_{LU,v} - \lambda_{phy} \cdot P_{ART}^*\end{aligned}\quad (8)$$

Free peptide, interstitial spaces:

Kidneys:

$$\begin{aligned}\frac{d}{dt} P_{K,int} &= -k_{on} \cdot P_{K,int} \cdot \frac{R_K}{V_{K,int}} + k_{off} \cdot RP_K + F_{fil} \left(\frac{P_{K,v}}{V_{K,v}} - \frac{P_{K,int}}{V_{K,int}} \right) + \lambda_{phy} \cdot P_{K,int}^* \\ \frac{d}{dt} P_{K,int}^* &= -k_{on} \cdot P_{K,int}^* \cdot \frac{R_K}{V_{K,int}} + k_{off} \cdot RP_K^* + F_{fil} \left(\frac{P_{K,v}^*}{V_{K,v}} - \frac{P_{K,int}^*}{V_{K,int}} \right) - \lambda_{phy} \cdot P_{K,int}^*\end{aligned}\quad (9)$$

Muscle, red marrow, skin, lungs, adipose tissue, heart, bone, rest and brain ($PS = 0$):

$$\begin{aligned}\frac{d}{dt} P_{i,int} &= PS_i \left(\frac{P_{i,v}}{V_{i,v}} - \frac{P_{i,int}}{V_{i,int}} \right) + \lambda_{phy} \cdot P_{i,int}^* \\ \frac{d}{dt} P_{i,int}^* &= PS_i \left(\frac{P_{i,v}^*}{V_{i,v}} - \frac{P_{i,int}^*}{V_{i,int}} \right) - \lambda_{phy} \cdot P_{i,int}^*\end{aligned}\quad (10)$$

Parotid, submandibular and lacrimal glands, tumour, kidneys, liver, spleen, GI and prostate:

$$\begin{aligned}\frac{d}{dt} P_{i,int} &= -k_{on} \cdot P_{i,int} \cdot \frac{R_i}{V_{i,int}} + k_{off} \cdot RP_i + PS_i \left(\frac{P_{i,v}}{V_{i,v}} - \frac{P_{i,int}}{V_{i,int}} \right) + \lambda_{phy} \cdot P_{i,int}^* \\ \frac{d}{dt} P_{i,int}^* &= -k_{on} \cdot P_{i,int}^* \cdot \frac{R_i}{V_{i,int}} + k_{off} \cdot RP_i^* + PS_i \left(\frac{P_{i,v}^*}{V_{i,v}} - \frac{P_{i,int}^*}{V_{i,int}} \right) - \lambda_{phy} \cdot P_{i,int}^*\end{aligned}\quad (11)$$

Further equations:

Peptide in kidney cells (unspecific)

$$\begin{aligned}\frac{d}{dt} P_{intra,K} &= \frac{P_{int,K}}{V_{int,K}} \cdot (F_{fil} - F_{ex}) - \frac{P_{intra,K}}{V_{intra,K}} \cdot (F_{fil} - F_{ex}) + \lambda_{phy} \cdot P_{intra,K}^* \\ \frac{d}{dt} P_{intra,K}^* &= \frac{P_{int,K}^*}{V_{int,K}} \cdot (F_{fil} - F_{ex}) - \frac{P_{intra,K}^*}{V_{intra,K}} \cdot (F_{fil} - F_{ex}) - \lambda_{phy} \cdot P_{intra,K}^*\end{aligned}\quad (12)$$

Bound to protein

$$\begin{aligned}\frac{d}{dt} PRP &= k_{PR} \cdot P_{VEN} + \lambda_{phy} \cdot PRP^* \\ \frac{d}{dt} PRP^* &= k_{PR} \cdot P_{VEN}^* - \lambda_{phy} \cdot PRP^*\end{aligned}\quad (13)$$

1 SUPPLEMENTAL TABLE A1 Parameter definition

Variable		Value	Unit	Source
k_{on}	association rate	0.046	$l \cdot nmol^{-1} \cdot min^{-1}$	(2) ^a
K_D	dissociation constant	1	$nmol \cdot l^{-1}$	(2) ^a
k_{off}	dissociation rate	$K_D \cdot k_{on}$	min^{-1}	
λ_{phy}	physical decay ¹⁷⁷ Lu and ⁶⁸ Ga	$7.15 \cdot 10^{-5} / 1.03 \cdot 10^{-2}$	min^{-1}	
BW	body weight	measured	kg	
BH	body height	measured	cm	
H	hematocrit	measured	unity	
F	flow total serum without tumour	$V_P \cdot 1.23 / min^b$	$l \cdot min^{-1}$	(3)
V_P	volume of total body serum	$2.8 \cdot (1 - H) \cdot BSA \cdot (l \cdot m^{-2})$	l	(4)
BSA	body surface area	$0.007184 \cdot BH^{0.725} \cdot BW^{0.425}$	m^2	(4)
ρ	assumed density for all organs and tumour	$1 ml \triangleq 1 g$		
Tumour				
$V_{TU,total}$	total volume of tumour 1 and 2	$V_{TU,total,0} \cdot e^{(\lambda_g \cdot \Delta T - \alpha_{TU} \cdot BED_{TU})}$	l	
$V_{TU,total,0}$	total volume of tumour 1 and 2 at time of PET/CT	measured	l	
ΔT	Elapsed time after first PET/CT	measured	min	
BED_{TU}	Biologically effective dose tumour	equation 2 manuscript	$Gy \alpha/\beta$	
α_{TU}	Radiosensitivity of tumour cells	fitted	Gy^{-1}	
λ_g	growth rate for androgen independent tumour cells	bone: $5.12 \cdot 10^{-6}$ lymph node: $3.85 \cdot 10^{-6}$	min^{-1}	(5)
$V_{TU,Rest,total}$	total volume of rest tumour time of therapy	$x_v \cdot V_{VOL,TU,Rest} \cdot e^{(\lambda_g \cdot \Delta T - \alpha_{TU} \cdot BED_{TU})}$ λ_g for bone was used	l	
$V_{TU,Rest,total,0}$	total volume of rest tumour time of PET	$x_v \cdot V_{VOL,TU,Rest}$	l	
$V_{VOL,TU,Rest}$	PET/CT volume with 15-20% SUV max	measured	l	
x_v	ratio between actual volume and PET/CT volume	Ratio derived from lesion 1 and 2	unity	
$V_{TU,int}$	interstitial space of tumour	$v_{TU,int} \cdot V_{TU,total}$	l	
$V_{TU,v}$	vascular space of tumour	$v_{TU,v} \cdot V_{TU,total}$	l	
$V_{TU,Rest,int}$	interstitial space of tumour remainder	$v_{TU,int} \cdot V_{TU,Rest,total}$	l	
$V_{TU,Rest,v}$	vascular space of tumour remainder	$v_{TU,v} \cdot V_{TU,Rest,total}$	l	
$v_{TU,int}$	interstitial space fraction of total tumour	0.38	unity	(6)
$v_{TU,v}$	vascular (serum) fraction of total tumour	$0.05 \cdot (1 - H)$	unity	(7)
F_{TU}	serum flow tumour	$f_{TU} \cdot V_{TU,total}$	$l \cdot min^{-1}$	
$F_{TU,Rest}$	serum flow tumour remainder	$f_{TU} \cdot V_{TU,Rest,total}$	$ml \cdot min^{-1}$	
f_{TU}	serum flow density tumour	fitted	$ml \cdot min^{-1} \cdot g^{-1}$	(7,8)
$f_{TU,Rest}$	serum flow density rest tumour	fitted	$ml \cdot min^{-1} \cdot g^{-1}$	

PS_{TU}	permeability surface area product tumour	$k_{TU} \cdot V_{TU,total}$	$ml \cdot min^{-1}$	
$PS_{TU,Rest}$	permeability surface area product tumour remainder	$k_{TU} \cdot V_{TU,Rest,total}$	$ml \cdot min^{-1}$	
k_{TU}	permeability surface area product tumour per unit mass (scaled for molecule size of PSMA I&T)	0.6 (maximal value from (6))	$ml \cdot min^{-1} \cdot g^{-1}$	(7)
$k_{TU,Rest}$	permeability surface area product tumour per unit mass (scaled for molecule size of PSMA I&T)	$k_{TU,Rest} = k_{TU}$	$ml \cdot min^{-1} \cdot g^{-1}$	
$[R_{TU,0}]$	PSMA receptor density	fitted	$nmol \cdot l^{-1}$	
$[R_{TU,Rest,0}]$	PSMA receptor density tumour remainder	$x_r \cdot ([R_{TU,1,0}] + [R_{TU,2,0}])/2$	$nmol \cdot l^{-1}$	(9)
x_r	ratio between actual and assumed receptor density of tumour remainder	1	unity	
$R_{TU,0}$	PSMA receptor number	$[R_{TU,0}] \cdot V_{TU,total}$	nmol	
$R_{TU,Rest,0}$	PSMA receptor number tumour remainder ^c	$[R_{TU,Rest,0}] \cdot V_{TU,Rest,total}$	nmol	
$\lambda_{TU,int}$	internalisation rate tumour	0.001	min^{-1}	(10)
$\lambda_{TU,release}$	release rate tumour	fitted	min^{-1}	
$\lambda_{TU,Rest,int}$	internalisation rate tumour remainder	0.001	min^{-1}	(10)
$\lambda_{TU,Rest,release}$	release rate tumour remainder	$(\lambda_{TU,1,release} + \lambda_{TU,2,release})/2$	min^{-1}	
Liver, spleen and kidneys				
$V_{L,total}$	volume total liver	CT measured	1	(11)
$V_{S,total}$	volume total spleen	CT measured	1	
$V_{K,total}$	volume total kidneys	CT measured	1	
$V_{i,v}$	vascular (serum) volume organ liver, spleen, kidneys	$V_{i,total} \cdot V_{i,v}$	1	
$V_{i,int}$	interstitial volume liver, spleen, kidneys	$V_{i,total} \cdot V_{i,int}$	1	
$V_{K,intra}$	volume intracellular kidneys	$(V_{K,total} - V_{K,int} - V_{K,v}) \cdot 2/3^d$	1	
$v_{L,v}$	vascular (serum) fraction liver	0.085	unity	(12)
$v_{S,v}$	vascular (serum) fraction spleen	0.12	unity	(12)
$v_{K,v}$	vascular (serum) fraction kidneys	0.055	unity	(12)
$v_{L,int}$	interstitial fraction liver	0.2	unity	(12)
$v_{S,int}$	interstitial fraction spleen	0.2	unity	(12)
$v_{K,int}$	interstitial fraction kidneys	0.15	unity	(12)
F_L	serum flow liver arterial	$0.065 \cdot F$	$l \cdot min^{-1}$	(3)
F_S	serum flow spleen	$0.03 \cdot F$	$l \cdot min^{-1}$	(3)
F_K	serum flow kidney	$f_k \cdot V_{K,total} \cdot (1-H)$	$l \cdot min^{-1}$	
f_k	age dependent blood flow to the kidney	$f_{k,C} - 0.026 \cdot Age$	$ml \cdot min^{-1} \cdot g^{-1}$	(13)
$f_{k,C}$	kidney blood flow, age independent factor for all ages	fitted	$ml \cdot min^{-1} \cdot g^{-1}$	
$\phi_{Therapy}$	ratio of sieving coefficients therapy	$\theta_{PSMA\ I\&T} / \theta_{Cr-51-EDTA} = 0.66$	unity	(14)
ϕ_{PET}	ratio of sieving coefficients PET/CT	$\theta_{PET} / \theta_{Cr-51-EDTA} = 0.75$		
GFR	glomerular filtration rate with ⁵¹ Cr-EDTA	$F_K \cdot x_k$	$l \cdot min^{-1}$	(15)
x_k	filtrated fraction of blood blow	fitted	unity	
F_{fil}	filtration	$GFR \cdot \phi_i^e$	$l \cdot min^{-1}$	
F_{ex}	excretion	$F_{fil} \cdot f_{ex}$	$l \cdot min^{-1}$	

f_{ex}	excretion fraction	0.96	unity	(16)
k_L	permeability surface area product per unit mass for liver	$k_{MUS} \cdot 100$	$\text{ml} \cdot \text{min}^{-1} \cdot \text{g}^{-1}$	(17)
k_S	permeability surface area product per unit mass for spleen	k_L (due to similar capillary structure)	$\text{ml} \cdot \text{min}^{-1} \cdot \text{g}^{-1}$	
$[R_{L,0}]$	receptor density liver	$[R_{PRO,0}] \cdot 0.05$	$\text{nmol} \cdot \text{l}^{-1}$	(18)
$[R_{S,0}]$	receptor density spleen	$[R_{K,0}] \cdot 0.2$	$\text{nmol} \cdot \text{l}^{-1}$	(18)
$[R_{K,0}]$	receptor density kidneys	fitted	$\text{nmol} \cdot \text{l}^{-1}$	
$\lambda_{L,int}$	internalization rate PSMA liver	$\lambda_{TU,int}$	min^{-1}	(19)
$\lambda_{S,int}$	internalization rate PSMA spleen	$\lambda_{TU,int}$	min^{-1}	(19)
$\lambda_{K,int}$	internalization rate PSMA kidneys	$\lambda_{TU,int}$	min^{-1}	(19)
$\lambda_{L,release}$	release rate liver	$\lambda_{K,release}$	min^{-1}	(16,20)
$\lambda_{S,release}$	release rate spleen	$\lambda_{K,release}$	min^{-1}	(16)
$\lambda_{K,release}$	release rate kidneys	fitted	min^{-1}	
Other organs				
$V_{PRO,total}$	volume total prostate (not removed for patients with prostatectomy)	$0.016 \cdot BW/71$	1	(21)
$V_{LU,total}$	volume total lungs	$1 \cdot BW/71$	1	(21)
$V_{SAL,total}$	volume total parotid gland	CT measured	1	
$V_{LAC,total}$	volume total lacrimal glands	CT measured	1	
$V_{SUB,total}$	volume total submandibular glands	CT measured	1	
$V_{MUS,total}$	volume total muscles	$30.078 \cdot BW/71$	1	(21)
$V_{GI,total}$	volume total GI + pancreas	$(0.385+0.548+0.104+0.15) \cdot BW/71$	1	(21)
$V_{SKIN,total}$	volume total skin	$3.408 \cdot BW/71$	1	(21)
$V_{ADL,total}$	volume total adipose tissue	$13.465 \cdot BW/71$	1	
$V_{RM,total}$	volume total red marrow	$1.1 \cdot BW/71$	1	(21)
$V_{BONE,total}$	volume total bone without red marrow	$10.165 \cdot BW/71 - V_{RM,total}$	1	(21)
$V_{HRT,total}$	volume total heart	$0.341 \cdot BW/71$	1	(21)
$V_{BR,total}$	volume total brain	$1.45 \cdot BW/71$	1	(21)
V_{BW}	volume of total body based on BW	$1 \text{ ml} \triangleq 1 \text{ g}$	1	
$V_{REST,total}$	volume of rest body $i = \text{all organs except tumour}$	$V_{BW} - \sum_i V_{i,total}$	1	
$V_{PRO,v}$	vascular volume prostate	$0.004 \cdot (1-H) \cdot V_{PRO,total}$	1	(6)
$V_{LU,v}$	vascular (serum) volume lungs	$0.105 \cdot V_P$	1	(3)
$V_{SAL,v}$	vascular (serum) volume parotid glands	$0.03 \cdot (1-H) \cdot V_{SAL,total}$	1	(22)
$V_{LAC,v}$	vascular (serum) volume lacrimal glands	$0.03 \cdot (1-H) \cdot V_{LAC,total}$		
$V_{SUB,v}$	vascular (serum) volume submandibular glands	$0.03 \cdot (1-H) \cdot V_{SUB,total}$		
$V_{MUS,v}$	vascular (serum) volume muscles	$0.14 \cdot V_P$	1	(3)
$V_{GI,v}$	vascular (serum) volume GI+ pancreas	$0.076 \cdot V_P$	1	(3)

$V_{SKIN,v}$	vascular(serum) volume skin	$0.03 \cdot V_P$	1	(3)
$V_{ADL,v}$	vascular(serum) volume adipose tissue	$0.05 \cdot V_P$	1	(3)
$V_{RM,v}$	vascular(serum) volume red marrow	$0.04 \cdot V_P$	1	(3)
$V_{BONE,v}$	vascular volume bone without red marrow	$0.07 \cdot V_P - V_{RM,v}$	1	(3)
$V_{HRT,v}$	vascular (serum) volume heart (supply)	$0.01 \cdot V_P$	1	(3)
$V_{BR,v}$	vascular(serum) volume brain	$0.012 \cdot V_P$	1	(3)
$V_{REST,v}$	serum volume rest i = all organs except tumour	$V_P - \sum_i V_{i,v}$	1	
V_{ART}	arterial serum plus ½ serum content of heart	$0.06 \cdot V_P + 0.045 \cdot V_P$	1	(3)
V_{VEN}	venous serum plus ½ serum content of heart	$0.18 \cdot V_P + 0.045 \cdot V_P$	1	(3)
$V_{PRO,int}$	interstitial fraction prostate	$0.25 \cdot V_{PRO,total}$	1	(6)
$V_{LU,int}$	interstitial fraction lungs	$V_{LU,v} \cdot \alpha_{LU}$	1	
$V_{SAL,int}$	interstitial fraction parotid glands	$0.23 \cdot V_{SAL,total}$	1	(22)
$V_{LAC,int}$	interstitial fraction lacrimal glands	$0.23 \cdot V_{LAC,total}$	1	
$V_{SUB,int}$	interstitial fraction submandibular glands	$0.23 \cdot V_{SUB,total}$	1	
$V_{MUS,int}$	interstitial fraction muscles	$V_{MUS,v} \cdot \alpha_{MUS}$	1	
$V_{GI,int}$	interstitial fraction GI+ pancreas	$V_{GI,v} \cdot \alpha_{GI}$	1	
$V_{SKIN,int}$	interstitial fraction skin	$V_{SKIN,v} \cdot \alpha_{SKIN}$	1	
$V_{ADL,int}$	interstitial fraction adipose tissue	$V_{ADL,v} \cdot \alpha_{ADI}$	1	
$V_{RM,int}$	interstitial fraction red marrow	$V_{RM,v} \cdot \alpha_{RM}$	1	
$V_{BONE,int}$	interstitial fraction bone without red marrow	$V_{BONE,v} \cdot \alpha_{BONE}$	1	
$V_{HRT,int}$	interstitial fraction heart	$V_{HRT,v} \cdot \alpha_{HRT}$	1	
$V_{REST,int}$	volume of rest body	$V_{REST,v} \cdot \alpha_{REST}$	1	
α_{MUS}	ratio of interstitial to vascular volume average man	$V_{MUS,int}/V_{MUS,v} = 5.9$	unity	(12)
α_{GI}	ratio of interstitial to vascular volume average man	$V_{GI,int}/V_{GI,v} = 8.8$	unity	(12)
α_{SKIN}	ratio of interstitial to vascular volume average man	$V_{SKIN,int}/V_{SKIN,v} = 8.9$	unity	(12)
α_{ADI}	ratio of interstitial to vascular volume average man	$V_{ADL,int}/V_{ADL,v} = 15.5$	unity	(12)
α_{RM}	ratio of interstitial to vascular volume average man	$V_{RM,int}/V_{RM,v} = 3.7$	unity	(12)
α_{HRT}	ratio of interstitial to vascular volume average man	$V_{HRT,int}/V_{HRT,v} = 3.7$	unity	(12)
α_{LU}	ratio of interstitial to vascular volume average man	$V_{LU,int}/V_{LU,v} = 5.5$	unity	(12)
α_{BONE}	ratio of interstitial to vascular volume average man	$V_{BONE,int}/V_{BONE,v} = 8.4$	unity	(12)
α_{REST}	ratio of interstitial to vascular volume average man	$V_{REST,int}/V_{REST,v} = 4.1$	unity	(12)
f_{PRO}	serum flow density prostate	$0.18 \cdot (1-H)$	$\text{ml} \cdot \text{min}^{-1} \cdot \text{g}^{-1}$	(6)
F_{PRO}	total serum flow to prostate	$f_{PRO} \cdot V_{PRO,total}$	$\text{ml} \cdot \text{min}^{-1}$	
f_{SAL}	serum flow density parotid glands	0.16	$\text{ml} \cdot \text{min}^{-1} \cdot \text{g}^{-1}$	(23)
F_{SAL}	total serum flow to parotid glands	$f_{SAL} \cdot V_{SAL,total}$	$\text{ml} \cdot \text{min}^{-1}$	
f_{LAC}	serum flow density lacrimal glands	f_{SAL}	$\text{ml} \cdot \text{min}^{-1} \cdot \text{g}^{-1}$	
F_{LAC}	total serum flow to lacrimal glands	$f_{LAC} \cdot V_{LAC,total}$	$\text{ml} \cdot \text{min}^{-1}$	

f_{SUB}	serum flow density submandibular glands	f_{SAL}	$\text{ml} \cdot \text{min}^{-1} \cdot \text{g}^{-1}$	
F_{SUB}	total serum flow to submandibular glands	$f_{\text{SUB}} \cdot V_{\text{SUB,tot}}$	$\text{ml} \cdot \text{min}^{-1}$	
F_{LU}	total serum flow lungs	F_{TOTAL}	$\text{ml} \cdot \text{min}^{-1}$	(3)
F_{MUS}	total serum flow to muscle	$0.17 \cdot F$	$\text{ml} \cdot \text{min}^{-1}$	(3)
F_{GI}	total serum flow to GI+ pancreas	$0.16 \cdot F$	$\text{ml} \cdot \text{min}^{-1}$	(3)
F_{SKIN}	total serum flow to skin	$0.05 \cdot F$	$\text{ml} \cdot \text{min}^{-1}$	(3)
F_{ADI}	total serum flow to adipose	$0.05 \cdot F$	$\text{ml} \cdot \text{min}^{-1}$	(3)
F_{RM}	total serum flow to red marrow (RM)	$0.03 \cdot F$	$\text{ml} \cdot \text{min}^{-1}$	(3)
F_{BONE}	total serum flow to bone (without RM)	$0.05 \cdot F$	$\text{ml} \cdot \text{min}^{-1}$	(3)
F_{HRT}	total serum flow to heart	$0.04 \cdot F$	$\text{ml} \cdot \text{min}^{-1}$	(3)
F_{BR}	total serum flow to brain	$0.12 \cdot F$	$\text{ml} \cdot \text{min}^{-1}$	(3)
F_{REST}	$i = \text{all organs except tumour}$	$F - \sum_i F_i$	$\text{ml} \cdot \text{min}^{-1}$	
F_{TOTAL}	total serum flow including tumour tissue	$F + F_{\text{TU},1} + F_{\text{TU},2} + F_{\text{TU,REST}}$	$\text{ml} \cdot \text{min}^{-1}$	
PS_i	permeability surface area product	$k_i \cdot V_{i,\text{total}}$	$\text{ml} \cdot \text{min}^{-1}$	
k_{PRO}	permeability surface area product per unit mass (scaled for molecule size of PSMA I&T) for prostate	0.1	$\text{ml} \cdot \text{min}^{-1} \cdot \text{g}^{-1}$	(6)
k_{LU}	permeability surface area product per unit mass for lungs	$k_{\text{MUS}} \cdot 100$	$\text{ml} \cdot \text{min}^{-1} \cdot \text{g}^{-1}$	(17)
k_{SAL}	permeability surface area product per unit mass for parotid glands	0.4	$\text{ml} \cdot \text{min}^{-1} \cdot \text{g}^{-1}$	(24)
k_{LAC}	permeability surface area product per unit mass for lacrimal glands	k_{SAL}	$\text{ml} \cdot \text{min}^{-1} \cdot \text{g}^{-1}$	
k_{SUB}	permeability surface area product per unit mass for submandibular glands	k_{SAL}	$\text{ml} \cdot \text{min}^{-1} \cdot \text{g}^{-1}$	
k_{MUS}	permeability surface area product per unit mass for muscle	0.02	$\text{ml} \cdot \text{min}^{-1} \cdot \text{g}^{-1}$	(17)
k_{GI}	permeability surface area product per unit mass for GI and pancreas	0.02 (assumed to similar to muscle)	$\text{ml} \cdot \text{min}^{-1} \cdot \text{g}^{-1}$	
k_{SKIN}	permeability surface area product per unit mass for skin	0.02 (assumed to similar to muscle)	$\text{ml} \cdot \text{min}^{-1} \cdot \text{g}^{-1}$	
k_{ADI}	permeability surface area product per unit mass for adipose	0.02 (assumed to similar to muscle)	$\text{ml} \cdot \text{min}^{-1} \cdot \text{g}^{-1}$	

k_{RM}	permeability surface area product per unit mass for red marrow	k_L (assumed to similar to liver)	$\text{ml} \cdot \text{min}^{-1} \cdot \text{g}^{-1}$	
k_{HRT}	permeability surface area product per unit mass for heart	0.02 (assumed to similar to muscle)	$\text{ml} \cdot \text{min}^{-1} \cdot \text{g}^{-1}$	
k_{BONE}	permeability surface area product per unit mass for bone	0.02 (assumed to similar to muscle)	$\text{ml} \cdot \text{min}^{-1} \cdot \text{g}^{-1}$	
k_{REST}	permeability surface area product per unit mass for rest	0.02 (assumed to similar to muscle)	$\text{ml} \cdot \text{min}^{-1} \cdot \text{g}^{-1}$	
$[R_{PRO,0}]$	receptor density prostate	$[R_{TU,Rest,0}] \cdot 110$	nmol l^{-1}	(23,25)
$[R_{SAL,0}]$	receptor density parotid glands	42	nmol l^{-1}	(23)
$[R_{LAC,0}]$	receptor density lacrimal glands	$[R_{SAL,0}]$	nmol l^{-1}	
$[R_{SUB,0}]$	receptor density submandibular glands	$[R_{SAL,0}]$	nmol l^{-1}	
$[R_{GI,0}]$	receptor density GI + pancreas	$[R_{PRO,0}] \cdot 0.06$	nmol l^{-1}	(18)
$\lambda_{NT,int}$	internalization rate for normal tissue	$\lambda_{TU,int}$	min^{-1}	(19)
$\lambda_{SAL,int}$	internalization rate for parotid glands	$\lambda_{TU,int}$	min^{-1}	
$\lambda_{LAC,int}$	internalization rate for lacrimal glands	$\lambda_{TU,int}$	min^{-1}	
$\lambda_{SUB,int}$	internalization rate for submandibular glands	$\lambda_{TU,int}$	min^{-1}	
$\lambda_{NT,release}$	degradation and release normal tissue (except salivary glands)	$\lambda_{K,release}$	min^{-1}	
$\lambda_{SAL,release}$	degradation and release parotid glands	0.00037	min^{-1}	(23)
$\lambda_{LAC,release}$	degradation and release lacrimal glands	$\lambda_{SAL,release}$	min^{-1}	
$\lambda_{SUB,release}$	degradation and release submandibular glands	$\lambda_{SAL,release}$	min^{-1}	
R	receptors free		nmol	
$R_{i,0}$	receptors total number of PSMA positive organ i	$[R_{i,0}] \cdot V_{i,total}$	nmol	
$[R_{i,0}]$	receptor density of PSMA positive organ i		nmol l^{-1}	
RP_i	peptide bound		nmol	
PRP	peptide bound to serum protein		nmol	
k_{PR}	binding rate peptide to serum	$4.7 \cdot 10^{-4}$	min^{-1}	(10)
$P_{i,intern}$	peptide internalized		nmol	
$P_{i,v}$	peptide free vascular		nmol	
$P_{i,int}$	peptide free interstitial		nmol	
$P_{K,intra}$	peptide intercellular kidneys		nmol	
P_{inj}	injected amount of unlabeled peptide	P1-5: 139; 91; 81; 67;294	nmol	
P_{inj}^*	injected amount of labeled peptide	P1-5: 8.4;7.5; 7.5;7.5;7.8	nmol	

1 ^aMean values from all measured (surface-plasmon-resonance-spectroscopy) ligands. The measured dissociation constant values are considerably lower than reported
2 in the literature. The values for the therapeutic (26) and PET ligand (27) are very similar. Using the K_D literature values (26,27), which were derived using
3 competitive cell binding ($K_D = 12$ nM) or enzyme based assays ($K_D = 7.5$ nM), for fitting the PBPK/PD model to human data, leads to inferior results (e.g. lower R^2
4 and higher AICc). Thus, it seems that k_{on} and k_{off} values determined using surface-plasmon-resonance-spectroscopy are more supported by human *in vivo* data.

5 ^bFor the average normal adult (blood) $F = 6500$ ml/min and $V = 5300$ ml. Therefore, a factor of 1.23 was assigned to account for the changes in total serum flow due
6 to volume changes.

7 ^cUsing the assumption of 266 nmol·l⁻¹ receptor density (9), 10^{12} cells per liter and 10 ml or 50 ml addition tumour volume.

8 ^dIt is assumed that 2/3 of the total intracellular volume of the kidneys is represented by the proximal tubular cells

9 ^eScaling of *GFR* due to different molecular sizes

10

1 **Absorbed dose (D) and biologically effective dose (BED):**

2 To calculate the absorbed dose (only self-dose was considered) and the BED of the kidneys and tumour the following equations and
3 parameter values (Table B) were used:

4
$$\dot{D}_i(t) = A_i(t) \cdot S_{i \leftarrow i} = A_{inj} \cdot a_i(t) \cdot S_{i \leftarrow i} \quad (14)$$

5
$$D_i(T) = \int_0^T \dot{D}_i(t) dt = A_{inj} \cdot \tilde{a}_i(T) \cdot S_{i \leftarrow i} \quad (15)$$

6 The BED (28) is defined as

7
$$BED_i = D_i \cdot \left(1 + \frac{G_i}{\alpha_i / \beta_i} \cdot D_i\right) \quad (16)$$

8 The factor G_i (Lea–Catcheside factor) (28) is defined as

9
$$G_i(T) = \frac{2}{D_i^2} \cdot \int_0^T \dot{D}_i(t) dt \cdot \int_0^t \dot{D}_i(\omega) \cdot e^{-\mu_i(t-\omega)} d\omega \quad (17)$$

10 Thus, after inserting Eq. (17) in (16) one obtains

11
$$BED_i = D_i + \frac{2 \cdot \int_0^T \dot{D}_i(t) dt \cdot \int_0^t \dot{D}_i(\omega) \cdot e^{-\mu_i(t-\omega)} d\omega}{\alpha_i / \beta_i} \quad (18)$$

12

13

14

1 **SUPPLEMENTAL TABLE A2**

Variable		Value	Unit	Source
$S_{K \leftarrow K}$	Dose factor kidneys to kidneys	$4.82 \cdot 10^{-6} \cdot 0.299 / V_{K, \text{total, measured}}$	$\text{Gy} \cdot \text{min}^{-1} \cdot \text{MBq}^{-1}$	(11)
$S_{\text{TU} \leftarrow \text{TU}}$	Dose factor tumour to tumour ^a	$S = 82.81 / (V_{\text{TU, total}} \cdot 1000) + 1.21 / (V_{\text{TU, total}} \cdot 1000)^{2/3} - 0.11 / (V_{\text{TU, total}} \cdot 1000)^{1/3}$	$\text{Gy} \cdot \text{min}^{-1} \cdot \text{MBq}^{-1}$	(29)
α/β_K	radiobiological parameters kidneys	2.5	Gy	(30)
μ_K	repair rate kidneys	$\ln(2)/60/2.8$	min^{-1}	(30)
α/β_{TU}	radiobiological parameters tumour	1.49	Gy	(31)
μ_{TU}	repair rate tumour	$\ln(2)/60/1.9$	min^{-1}	
\bar{a}_i	time-integrated activity coefficient of organ i		h	
a_i	fraction of administered activity of organ i		unity	
D_i	dose to organ i		Gy	
\dot{D}_i	dose rate to organ i		$\text{Gy} \cdot \text{min}^{-1}$	
T	Integration time	30000	min	
G_i	Lea–Catchside factor of organ i		unity	(32)
BED_i	biologically effective dose to organ i		Gy	(32)

2

3 ^aThe function $S = A/(V_{\text{TU, total}} \cdot 1000) + B/(V_{\text{TU, total}} \cdot 1000)^{2/3} - C/(V_{\text{TU, total}} \cdot 1000)^{1/3}$ (valid for tumours > 1 ml) was fitted to the OLINDA data for ¹⁷⁷Lu spheres.

References

1. Rippe B, Haraldsson B. Fluid and protein fluxes across small and large pores in the microvasculature. Application of two-pore equations. *acta Physiol Scand.* 1987;131:411-428.
2. Winter G, Drescher A, Baur B, Solbach C, Reske SN, Beer AJ. Comparative analysis of chelator-modified peptides for imaging of prostate carcinoma. *Annual Congress EANM.* 2014.
3. Leggett RW, Williams LR. A proposed blood circulation model for reference man. *Health Phys.* 1995;69:187-201.
4. Buchmann I, Kull T, Glatting G, et al. A comparison of the biodistribution and biokinetics of ^{99m}Tc-anti-CD66 mAb BW 250/183 and ^{99m}Tc-anti-CD45 mAb YTH 24.5 with regard to suitability for myeloablative radioimmunotherapy. *Eur J Nucl Med Mol Imaging.* 2003;30:667-673.
5. Berges RR, Vukanovic J, Epstein JI, et al. Implication of cell kinetic changes during the progression of human prostatic cancer. *Clin Cancer Res.* 1995;1:473-480.
6. Buckley DL, Roberts C, Parker GJ, Logue JP, Hutchinson CE. Prostate cancer: evaluation of vascular characteristics with dynamic contrast-enhanced T1-weighted MR imaging--initial experience. *Radiology.* 2004;233:709-715.
7. Luczynska E, Heinze-Paluchowska S, Blecharz P, et al. Correlation between CT perfusion and clinico-pathological features in prostate cancer: a prospective study. *Med Sci Monit.* 2015;21:153-162.
8. Franiel T, Lüdemann L, Rudolph B, et al. Prostate MR imaging: tissue characterization with pharmacokinetic volume and blood flow parameters and correlation with histologic parameters. *Radiology.* 2009;252:101-108.
9. Wang X, Ma D, Olson WC, Heston WD. In vitro and in vivo responses of advanced prostate tumors to PSMA ADC, an auristatin-conjugated antibody to prostate-specific membrane antigen. *Mol Cancer Ther.* 2011;10:1728-1739.
10. Kletting P, Kull T, Maass C, et al. Optimized Peptide Amount and Activity for ⁹⁰Y-Labeled DOTATATE Therapy. *J Nucl Med.* 2016;57:503-508.
11. Stabin MG, Sparks RB, Crowe E. OLINDA/EXM: The Second-Generation Personal Computer Software for Internal Dose Assessment in Nuclear Medicine. *J Nucl Med.* 2005;46:1023-1027.
12. Shah DK, Betts AM. Towards a platform PBPK model to characterize the plasma and tissue disposition of monoclonal antibodies in preclinical species and human. *J Pharmacokinet Pharmacodyn.* 2012;39:67-86.
13. Hollenberg NK, Adams DF, Solomon HS, Rashid A, Abrams HL, Merrill JP. Senescence and the renal vasculature in normal man. *Circ Res.* 1974;34:309-316.

- 1 **14.** Schmidt MM, Wittrup KD. A modeling analysis of the effects of molecular size and binding affinity on tumor targeting. *Mol Cancer Ther.* 2009;8:2861-
2 2871.
3
- 4 **15.** Fresco GF, DiGiorgio F, Curti GL. Simultaneous estimation of glomerular filtration rate and renal plasma flow. *J Nucl Med.* 1995;36:1701-1706.
5
- 6 **16.** Kletting P, Muller B, Erentok B, et al. Differences in predicted and actually absorbed doses in peptide receptor radionuclide therapy. *Med Phys.*
7 2012;39:5708-5717.
8
- 9 **17.** Groothuis DR. The blood-brain and blood-tumor barriers: a review of strategies for increasing drug delivery. *Neuro Oncol.* 2000;2:45-59.
10
- 11 **18.** O'Keefe DS, Bacich DJ, Heston WD. Comparative analysis of prostate-specific membrane antigen (PSMA) versus a prostate-specific membrane antigen-
12 like gene. *Prostate.* 2004;58:200-210.
13
- 14 **19.** Antunes P, Ginj M, Zhang H, et al. Are radiogallium-labelled DOTA-conjugated somatostatin analogues superior to those labelled with other radiometals?
15 *Eur J Nucl Med Mol Imaging.* 2007;34:982-993.
16
- 17 **20.** Velikyan I, Sundin A, Eriksson B, et al. In vivo binding of [⁶⁸Ga]-DOTATOC to somatostatin receptors in neuroendocrine tumours--impact of peptide mass.
18 *Nucl Med Biol.* 2010;37:265-275.
19
- 20 **21.** Snyder WS, Cook MJ, Nasset ES, Karhausen RS, Howells GP. *Report of the Task Group on Reference Man. ICRP publication 23.* Oxford: Elsevier; 1975.
21
- 22 **22.** Berggreen E, Wiig H. Lowering of interstitial fluid pressure in rat submandibular gland: a novel mechanism in saliva secretion. *Am J Physiol Heart Circ*
23 *Physiol.* 2006;290:H1460-1468.
24
- 25 **23.** Kletting P, Schuchardt C, Kulkarni HR, et al. Investigating the Effect of Ligand Amount and Injected Therapeutic Activity: A Simulation Study for ¹⁷⁷Lu-
26 Labeled PSMA-Targeting Peptides. *PLoS One.* 2016;11:e0162303.
27
- 28 **24.** Rumboldt Z, Al-Okaili R, Deveikis JP. Perfusion CT for head and neck tumors: pilot study. *AJNR Am J Neuroradiol.* 2005;26:1178-1185.
29
- 30 **25.** Ben Jemaa A, Bouraoui Y, Sallami S, et al. Co-expression and impact of prostate specific membrane antigen and prostate specific antigen in prostatic
31 pathologies. *J Exp Clin Cancer Res.* 2010;29:171.
32
- 33 **26.** Weineisen M, Schottelius M, Simecek J, et al. ⁶⁸Ga- and ¹⁷⁷Lu-Labeled PSMA I&T: Optimization of a PSMA-Targeted Theranostic Concept and First
34 Proof-of-Concept Human Studies. *J Nucl Med.* 2015;56:1169-1176.
35
- 36 **27.** Eder M, Schafer M, Bauder-Wust U, et al. ⁶⁸Ga-complex lipophilicity and the targeting property of a urea-based PSMA inhibitor for PET imaging.
37 *Bioconjug Chem.* 2012;23:688-697.
38
- 39 **28.** Hobbs RF, Sgouros G. Calculation of the biological effective dose for piecewise defined dose-rate fits. *Med Phys.* 2009;36:904-907.
40

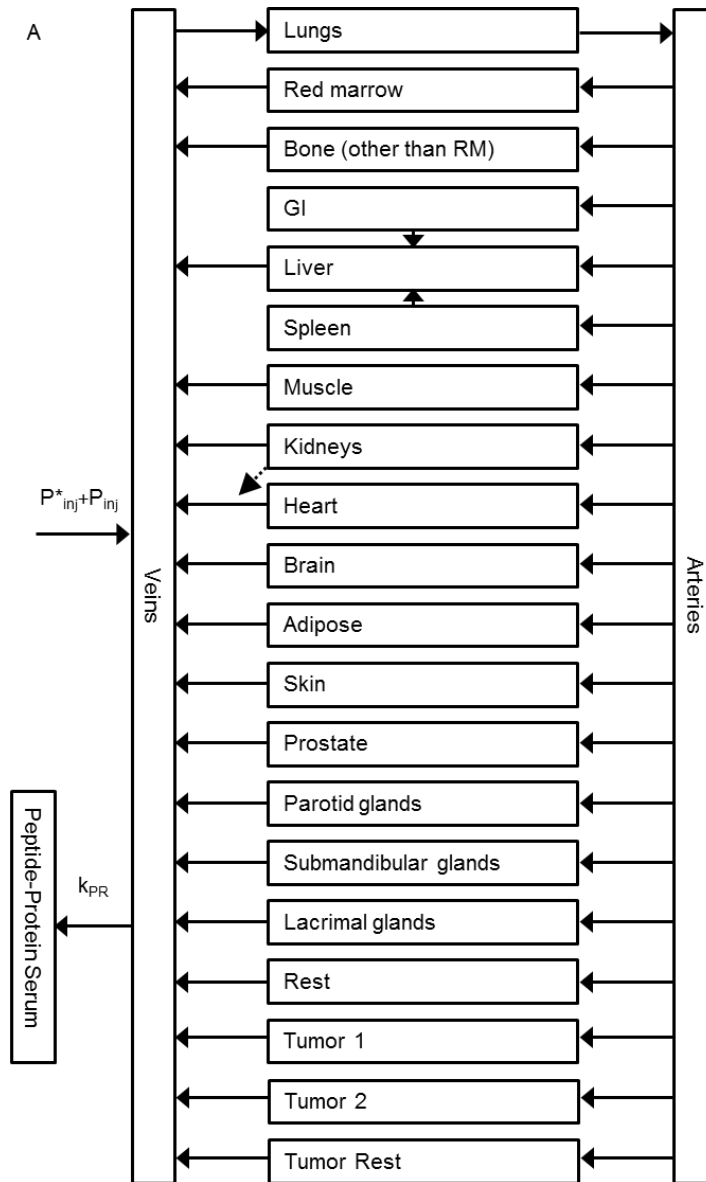
- 1 **29.** Stabin MG, Siegel JA. Physical models and dose factors for use in internal dose assessment. *Health Phys.* 2003;85:294-310.
2
3 **30.** Cremonesi M, Botta F, Di Dia A, et al. Dosimetry for treatment with radiolabelled somatostatin analogues. A review. *Q J Nucl Med Mol Imaging.*
4 2010;54:37-51.
5
6 **31.** Fowler J, Chappell R, Ritter M. Is alpha/beta for prostate tumors really low? *International Journal of Radiation Oncology Biology Physics.* 2001;50:1021-
7 1031.
8
9 **32.** Konijnenberg M. From imaging to dosimetry and biological effects. *Q J Nucl Med Mol Imaging.* 2011;55:44-56.
10
11

1 **PBPK Model compartments**

2

3

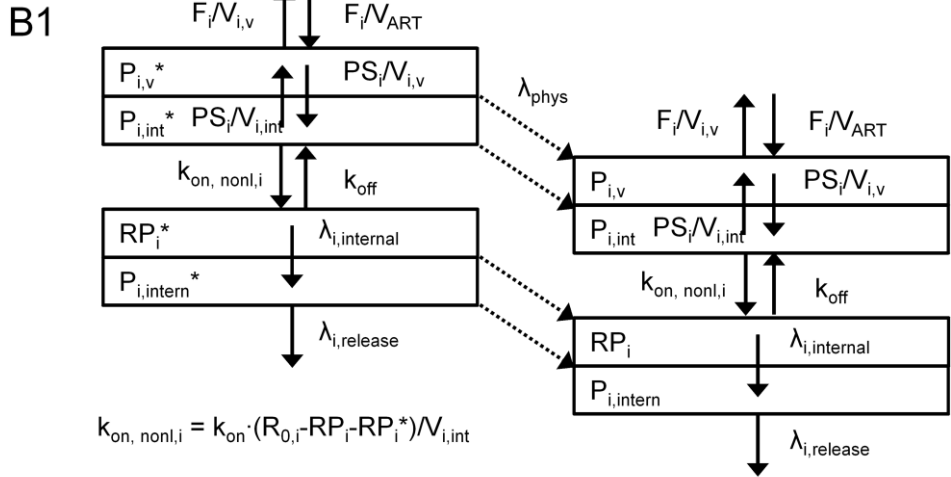
A



1
2

1
2
3
4
5
6
7

Supplemental Figure A. Main model structure: All organs are represented by a rectangular compartment and connected via the serum flow. Each organ within this model, except arteries, veins, brain and protein serum, is divided into sub-compartments. The substance is cleared via the kidneys. The compartment “Peptide-Protein serum” contains peptide bound to serum protein. As the fraction of bound peptide to proteins is small compared to the total amount and to reduce complexity, only the „veins“ were connected to this compartment. The corresponding fraction for each specific organ is considered in the fitting process by assigning the data to the specific compartments.

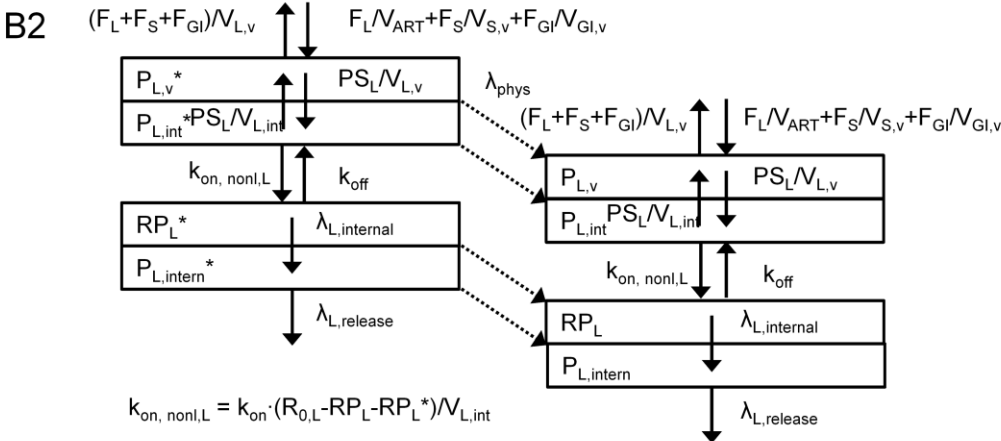


8
9
10
11
12
13
14
15
16
17
18

Supplemental Figure B1. GI, spleen, prostate, submandibular, lacrimal and parotid glands and tumour: The entire model consists of three systems, one for labelled (with *) and one for unlabelled peptide. The systems are connected by the competition for free receptors ($k_{on,nonl,i} = k_{on} \cdot (R_{0,i} - RP_i - RP_i^*) / V_{i,int}$) and by physical decay (λ_{phys}). All physiological parameters are assumed to be equal for the labelled and unlabelled substance.

k_{off} is the dissociation rate, the transport of peptide via serum flow to organ i is described by $F_i/V_{i,v}$ (where F_i is serum flow and $V_{i,v}$ is serum volume of the arteries), $F_i/V_{i,v}$ describes the transport of peptide via serum flow out of organ and (where F_i is serum flow and $V_{i,v}$ is serum volume of the respective organ, RP_i is PSMA-specific bound peptide to the cell surface, $R_{0,i}$ and RP_i is free peptide of the

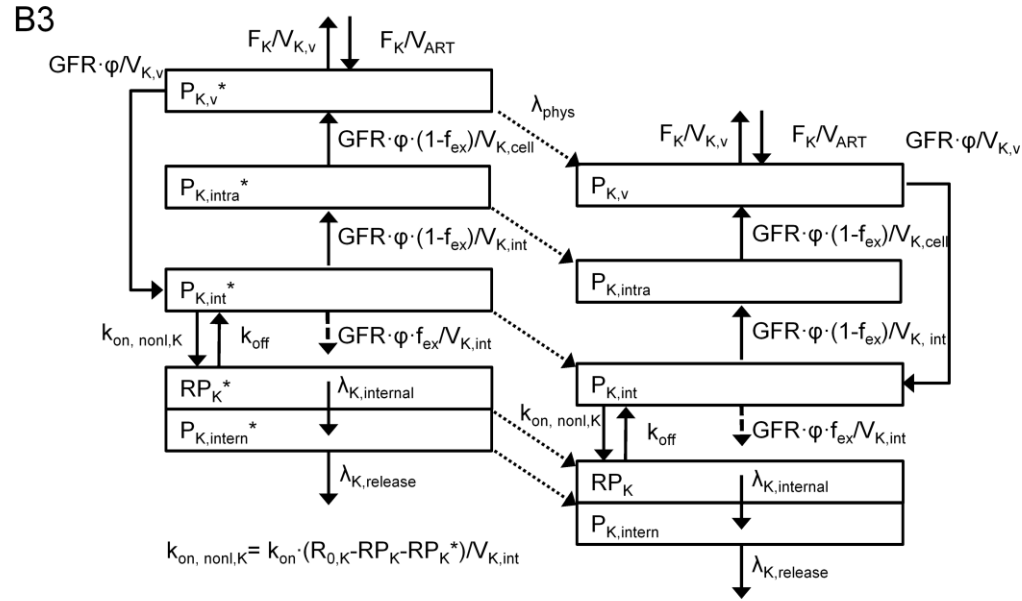
1
2
3
4
5
6
7
8
9
10
11
12
13



14
15
16
17
18
19

Supplemental Figure B2. Liver: For the liver the model description of B1 applies but the serum flow is composed of liver arterial, GI and spleen flow.

1



2

3

4

5

6

7

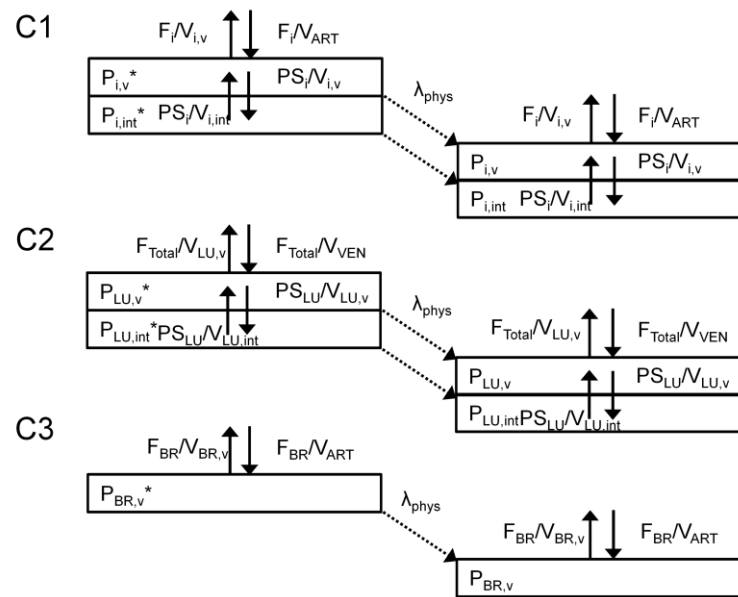
8

9

10

11

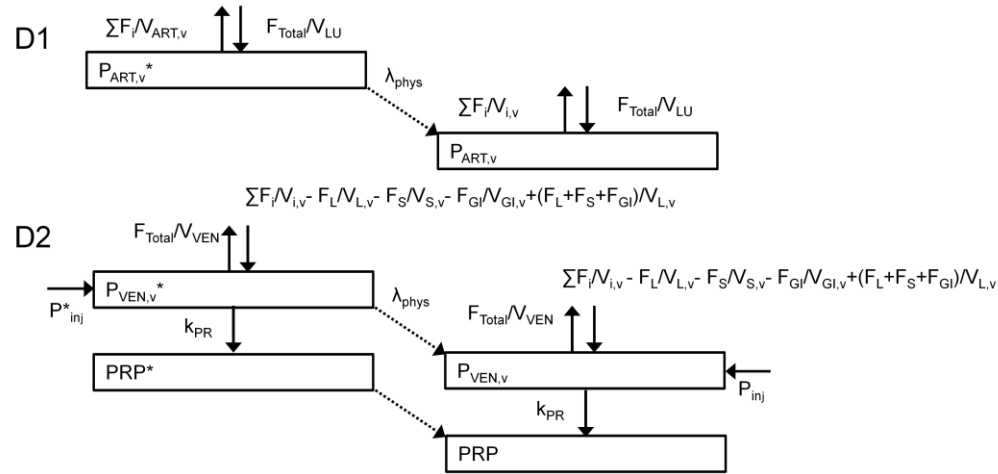
Supplemental Figure B3. Kidneys: The peptide is transported via serum flow to the vascular compartment then filtrated into the interstitial part. Due to the administration of amino acids the largest fraction ($f_{ex} = 0.96$) of peptide is excreted. All unspecific uptake mechanisms are modelled with flow $GFR \cdot \phi \cdot (1 - f_{ex})$ in and out of kidney cells. GFR was measured with Cr-51-EDTA.



1
2
3
4
5
6
7
8

Supplemental Figure C. PSMA negative tissue and brain: For adipose, bone (other than red marrow), skin, heart (C1) and lung (C2) the model on the organ level simplifies to the transport of peptide via serum flow and transcapillary extravasation. For brain (C3) the model reduces to serum flow.

1
2



3
4
5
6
7
8

Supplemental Figure D. Arteries and veins: As the fraction of bound peptide to proteins (*PRP*) is small compared to the total amount and to reduce complexity, only the „veins (D2)“ were connected to *PRP*. The corresponding fraction for each specific organ is considered in the fitting process by assigning the data to the specific compartments.

B. Background corrections

Assigning tumour data from planar scintigraphy to model compartments

For fitting the model parameters to the data derived from the therapeutic planar images, the following equation was used to assign the tumour data to the compartments of the PBPK model:

$$a_{TU,Therapy}(t) = \frac{\left[P_{TU,v}^*(t) + P_{TU,int}^*(t) + RP_{TU}^*(t) + P_{TU,intern}^*(t) + \frac{(A_{ROI,TU} \cdot h_{PET,TU})}{(V_{MUS,total} + V_{ADI,total})} (P_{MUS,v}^*(t) + P_{MUS,int}^*(t) + P_{ADI,v}^*(t) + P_{ADI,int}^*(t)) \right]}{amount_{injected,thera} \cdot f_{hot,thera}} \quad (B.1)$$

Where $a(t)$ is the fraction of administered activity of a specific tumour ROI, $amount_{injected}$ the total injected therapy amount, f_{hot} is the fraction of labelled peptide, $A_{ROI,TU}$ is the area of the drawn ROI in the planar image, $h_{PET,TU}$ is the patient thickness (minus tumour diameter) at the particular location of the tumour measured in the PET/CT image, $V_{MUS,total}$ and $V_{ADI,total}$ is the total muscle and adipose volume (Supplement A) and $P_{TU,v}^*(t) + P_{TU,int}^*(t) + RP_{TU}^*(t) + P_{TU,intern}^*(t)$ are the amount of labelled peptide in the vascular, interstitial, bound and internalized tumour compartment, respectively. $P_{MUS,v}^*(t)$, $P_{MUS,int}^*(t)$, $P_{ADI,v}^*(t)$ and $P_{ADI,int}^*(t)$ describe the amount of labelled peptide in the vascular and interstitial spaces of muscle and adipose tissue, respectively. For tumour dose calculation only compartments pertaining to the tumour were used. The fraction of peptide bound to blood pool protein was neglected.

Assigning tumour data from PET/CT to model compartments

For fitting the model parameters to the data derived from the pre-therapeutic PET/CT images, the following equation was used to assign the data to the compartments of the PBPK model:

$$a_{TU,PET}(t) = \frac{\left[P_{TU,v}^*(t) + P_{TU,int}^*(t) + RP_{TU}^*(t) + P_{TU,intern}^*(t) + \frac{(V_{VOL,TU,2} - V_{VOL,TU,1})}{(V_{MUS,total} + V_{ADI,total})} (P_{MUS,v}^*(t) + P_{MUS,int}^*(t) + P_{ADI,v}^*(t) + P_{ADI,int}^*(t)) \right]}{amount_{injected,PET} \cdot f_{hot,PET}} \quad (B.2)$$

Where $V_{VOL,TU,1}$ is the estimated volume using the pre-therapeutic PET image with an threshold of 20-50% so that the CT tumour volume and the PET match. $V_{VOL,TU,2}$ is the estimated volume using the pre-therapeutic PET image with an threshold of 10-20% leading to a 5 mm larger radius (i.e. one voxel) that for $V_{VOL,TU,2}$ to get all activity contained in the tumour. The activity derived using $V_{VOL,TU,2}$ was used as data point $a_{TU,PET}(t)$ and was indirectly background corrected using the above described data assignment.

Assigning REST tumour data from PET/CT to model compartments

For tumour remainder (rest), the following equation was used in the fitting of model parameters to the data derived from the pre-therapeutic PET/CT images:

$$a_{TU,Rest,PET}(t) = \frac{\left[P_{TU,Rest,v}^*(t) + P_{TU,Rest,int}^*(t) + RP_{TU,Rest}^*(t) + P_{TU,Rest,intern}^*(t) + \frac{V_{VOL,TU,Rest} (1-x_v)}{(V_{MUS,total} + V_{ADI,total})} (P_{MUS,v}^*(t) + P_{MUS,int}^*(t) + P_{ADI,v}^*(t) + P_{ADI,int}^*(t)) \right]}{amount_{injected,PET} \cdot f_{hot,PET}} \quad (B.3)$$

$a_{TU,Rest,PET}(t)$ was derived with an threshold of 15-20%. Where x_v is the correction factor to get the actual tumour volume (this information is derived from two tumour lesions). x_v P1-13: 0.62,0.55,0.67,0.55,0.53,0.58,0.61,0.72,0.44,0.34,0.35,0.62,0.55.

Assigning kidney data from PET/CT to model compartments

$$a_{K,PET}(t) = \frac{\left[P_{K,v}^*(t) + P_{K,int}^*(t) + RP_K^*(t) + P_{K,intern}^*(t) + P_{K,v}^*(t) + \frac{(V_{VOL,K} - V_{K,total})}{(V_{MUS,total} + V_{ADI,total})} (P_{MUS,v}^*(t) + P_{MUS,int}^*(t) + P_{ADI,v}^*(t) + P_{ADI,int}^*(t)) \right]}{amount_{injected,PET} \cdot f_{hot,PET}} \quad (B.4)$$

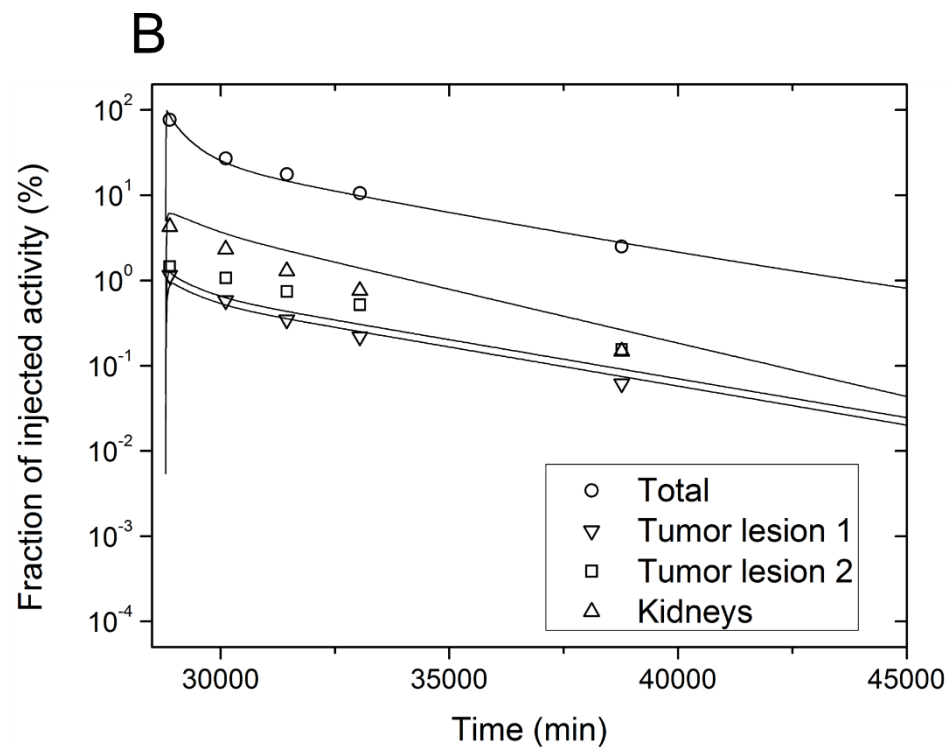
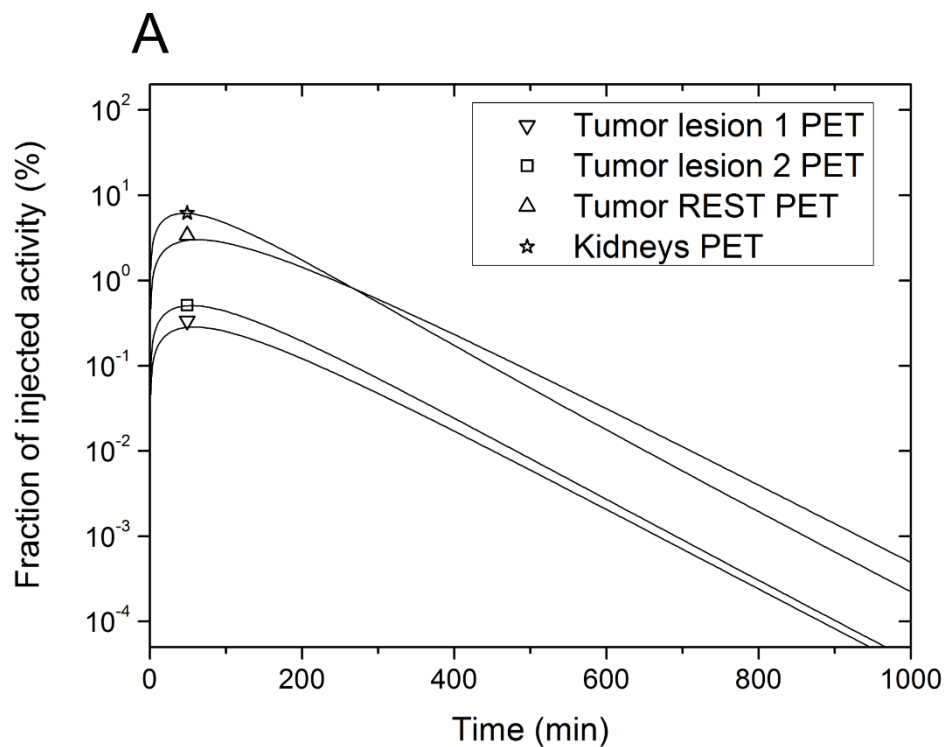
Where $V_{VOL,K}$ is the volume used for activity quantification with an threshold of 10-20% leading to a 5 mm larger radius (i.e. one voxel) than that of the kidney volume, $V_{K,total}$, estimated using the CT.

SUPPLEMENTAL TABLE B1. Patients measurement time post injection

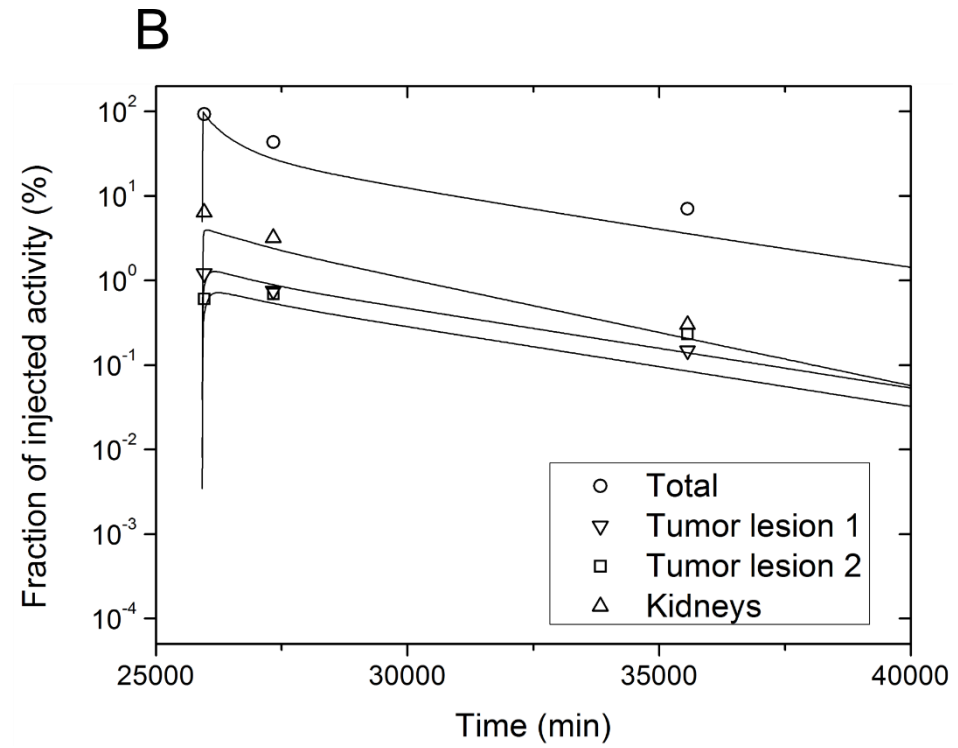
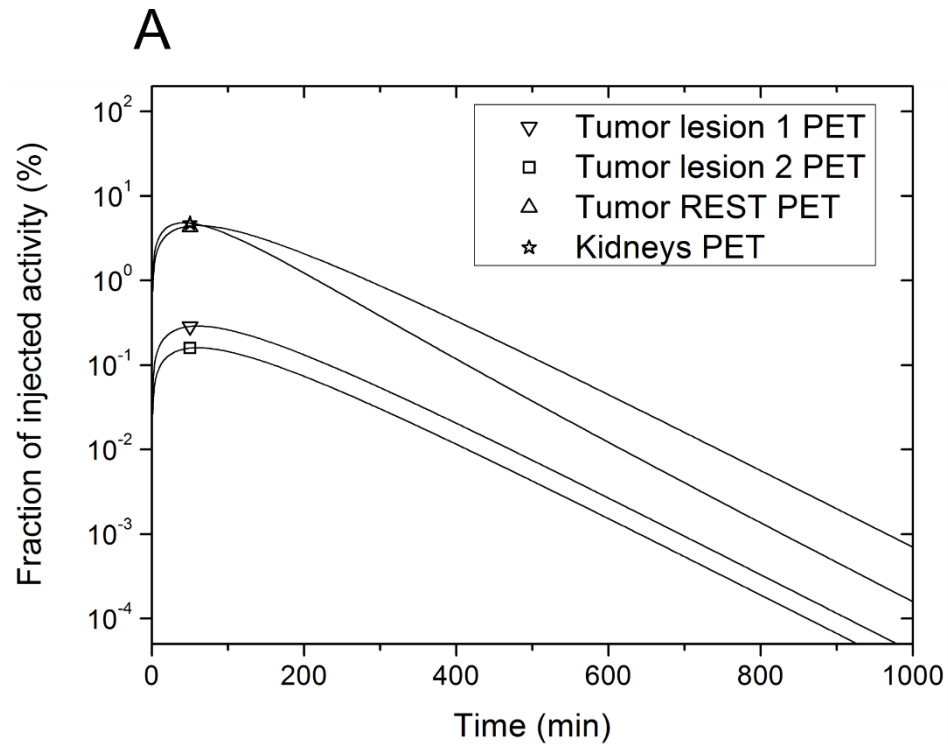
Patient no.	Measurement times (h)				
P1	1.1	22	44	70	166
P2	1.3	18		66	163
P3	0.5	18	46	68	165
P4	2.2	19	47	67	164
P5	0.3	23			160
P6	0.3	21			164
P7	2.1	25			163
P8	0.4	22			167
P9	0.6	20			165
P10	0.2	20			162
P11	0.3	18			162
P12	0.3	21			163
P13	0.2	17			161

C.

SUPPLEMENTAL FIGURE C1. Example of typical fit (P1): PET (A) and therapy (B)



SUPPLEMENTAL FIGURE C2. Fits of P5 (lowest R^2): PET (A) and therapy (B)



SUPPLEMENTAL TABLE C1. Averaged estimated pharmacokinetic parameters of leave-one-out jackknife populations (PSA positive patients)

Quantity	Organ	Parameter	Unit	Mean	SD	Literature
PSMA receptor density	Kidneys	$[R_{K,0}]$	$\text{nmol}\cdot\text{l}^{-1}$	16	4.3	-
	Tumor lesion	$[R_{TU,0}]$		45	28	16-160*
	Tumor REST	$[R_{TU,Rest,0}] = ([R_{TU,1,0}] + [R_{TU,2,0}])/2$				
Release rate	Kidneys	$\lambda_{K,release}$	min^{-1}	2.2×10^{-4}	6.0×10^{-5}	$0.5 - 2.3 \times 10^{-4}^\dagger$
	Tumor	$\lambda_{TU,release}$	min^{-1}	1.4×10^{-4}	6.0×10^{-5}	$0.0 - 3 \times 10^{-4}^\dagger$
Serum flow density	Tumor lesion	$f_{TU,0}$	$\text{ml}\cdot\text{min}^{-1}\cdot\text{g}^{-1}$	0.14	0.12	0.1 [‡]
	Tumor REST	$f_{TU,Rest}$	$\text{ml}\cdot\text{min}^{-1}\cdot\text{g}^{-1}$	0.06	0.034	
	Kidneys	$f_K = f_{K,C} - 0.026\cdot\text{Age}$ $f_{K,C}$	$\text{ml}\cdot\text{min}^{-1}\cdot\text{g}^{-1}$ $\text{ml}\cdot\text{min}^{-1}\cdot\text{g}^{-1}$	4.0	0.39	4.3 [§]

Each patient file was fitted separately using an iterative fitting. After each iteration, the mean and standard deviation were obtained and used as Bayesian information in the next step, until convergence. The pharmacokinetic information of the remaining tumor is contained in the total body scan and the PET measurement.

* Assuming densities of 10^8 - 10^9 cells/ml [1] and 100.000 copies/cell [2]

† Derived using a PBPK for a sst2 specific ^{111}In labeled ligand [3]

‡ Normally tumor blood flow ranges between 0.01-1.0 $\text{ml}\cdot\text{min}^{-1}\cdot\text{g}^{-1}$. 0.1 $\text{ml}\cdot\text{min}^{-1}\cdot\text{g}^{-1}$ is often used as typical e.g. for simulations studies [4]

§ [5]

SUPPLEMENTAL TABLE C2. Coefficients of determination R^2 of the fits of total body, tumor lesion 1, tumor lesion 2 and the kidneys of all patients (without P7).

Patient no.	Coefficient of determination R^2			
	Total body	Tumor lesion 1	Tumor lesion 2	Kidneys
P1	0.98	1.00	1.00	1.00
P2	0.89	1.00	1.00	1.00
P3	0.73	1.00	1.00	1.00
P4	0.80	0.99	0.98	1.00
P5	0.91	0.77	0.40	0.94
P6	0.99	0.89	0.99	0.88
P8	0.96	0.94	0.99	1.00
P9	1.00	0.92	0.81	0.98
P10	0.99	0.87	0.97	1.00
P11	0.94	0.84	0.91	1.00
P12	0.94	0.95	0.86	0.92
P13	0.98	0.86	0.95	0.98

REFERENCES

1. Del Monte, U., *Does the cell number 10(9) still really fit one gram of tumor tissue?* Cell Cycle, 2009. **8**(3): p. 505-6.
2. Wang, X., et al., *In vitro and in vivo responses of advanced prostate tumors to PSMA ADC, an auristatin-conjugated antibody to prostate-specific membrane antigen.* Mol Cancer Ther, 2011. **10**(9): p. 1728-39.
3. Kletting, P., et al., *Optimized Peptide Amount and Activity for ⁹⁰Y-Labeled DOTATATE Therapy.* J. Nucl. Med., 2016. **57**(4): p. 503-508.
4. Thurber, G.M. and R. Weissleder, *A Systems Approach for Tumor Pharmacokinetics.* PLoS ONE, 2011. **6**(9): p. e24696.
5. Hollenberg, N.K., et al., *Senescence and the renal vasculature in normal man.* Circ Res, 1974. **34**(3): p. 309-16.